by Yi-Gang Xu[1], Bin He[1], Xiaolong Huang[1], Zhenyu Luo[1], Sun-Lin Chung[2], Long Xiao[3], Dan Zhu[1], Hui Shao[1], Wei-Ming Fan[1], Jifeng Xu[1], and Yue-Jun Wang[1]

Identification of mantle plumes in the Emeishan Large Igneous Province

1 Key Laboratory of Isotope Geochronology and Geochemistry, Guangzhou Institute of Geochemistry, Chinese Academy of Sciences, 510640 Wushan, Guangzhou, China. *E-mail: yigangxu@gig.ac.cn*
2 Department of Geosciences, National Taiwan University, Taipei 10699, Taiwan, China
3 China University of Geosciences, Wuhan 430074, China

The plume hypothesis has been recently challenged largely because some fundamental aspects predicted by the modeling of plumes are found to be lacking in some classic hotspot regions. This review paper summarizes recent achievements made in the late Permian Emeishan continental flood basalt province in southwest China. Data from various disciplines are evaluated by comparing observation against prediction of the plume hypothesis. It is shown that 7 out of the 9 most convincing arguments in support of mantle plumes are found in the Emeishan large igneous province (LIP). In particular, sedimentological data show unequivocal evidence for a lithospheric doming event prior to the Emeishan volcanism. This observation, the presence of high-temperature magmas, emplacement of immense volume of magmas over a short time span and the spatial variation in basalt geochemistry are all consistent with predictions of plume modeling, thus providing strong support for the validity of the mantle plume hypothesis.

Introduction

The plume hypothesis has been widely adopted to explain the formation of age-progressive volcanic chain hotspots such as Hawaii and large igneous provinces (LIP) in both oceanic and continental settings (e.g., Morgan, 1971, White and McKenzie, 1989; Campbell and Griffiths, 1990; Coffin and Eldholm, 1994). But it is now challenged because some fundamental aspects predicted by the modeling of plumes are found to be lacking in some classic regions like Iceland and Yellowstone (Foulger et al., 2000; Christiansen et al., 2002). For instance, a primary implication of the hotspot hypothesis is the fixity of deep-seated mantle plume, which is in contrast to the overlying plates that move at rates up to 100 mm/yr. This allowed the development of a “hotspot reference frame” that has been used for tectonic and paleogeographic studies (e.g., Besse and Courtillot, 2002). However, recent paleomagnetic studies indicate that the Hawaiian hotspot has not been fixed (Tarduno et al., 2003). This is further confirmed by mantle convection computation which shows that plumes should not be fixed, but instead are distorted by mantle flow (Steinberger et al., 2004). On the other hand, plume theory is based on the premise that hot material rises up from the mantle, above or below the 660 km discontinuity, to feed hotspots on the surface (White and McKenzie, 1989; Campbell and Griffiths, 1990), as such plumes are thought of as “bottom-up” phenomena. However, in Iceland and Yellowstone, researchers are more inclined to a “top-down” hypothesis, in which shallow lithospheric processes may fuel melt production (Anderson, 2000; Foulger, 2002; Christiansen et al., 2002). It is now clear that there is not a plume in every hotspot, and that there may be distinctive types of hotspots rising from different levels of the Earth's interior (Courtillot et al., 2003). The plume debate continues (DePaolo and Manga, 2003; Foulger and Natland, 2003; Anderson, 2003; Montelli et al., 2004), with controversy arising from whether or not the current resolution of seismic data is sufficient to detect small thermal anomalies such as mantle plumes (Kerr et al., 2005). These controversies highlight the demand for refining the plume hypothesis or testing it against observations (Campbell, 2001; Campbell and Davies, 2006). So far, considerable efforts have been made in this direction in the oceanic setting (see IODP reports), but are still not sufficient in the continental setting.

Courtillot et al. (2003) lists five criteria commonly used to identify mantle plumes in modern, active hotspots. Among these criteria, a deep mantle tomographic signal is the key. However, seismic technique has limited application in identifying ancient plumes, because geophysics only provides us with a snapshot of the present-day Earth's structure. A thoughtful review on how to identify ancient mantle plumes is provided by Campbell (2001) who suggests pre-volcanic uplift, radiating dyke swarm, physical volcanology, hotspot tracks and geochemical characteristics of plume-derived basalts as key identifying criteria. These geological consequences associated with thermal anomalies, and a number of testable predictions of plume hypothesis (including dimension of large igneous province, high-temperature magmas and plume structure) are the clues to tracing ancient plumes. In practice, identification of ancient mantle plumes requires the combined application of a range of criteria (Campbell, 2001; 2005).

In recent years, the Emeishan basalts in southwest China have attracted the attention of the scientific community because of possible synchrony with the eruption of the Siberian Traps, and, as such, its possible relationship to mass extinctions during the Late Permian (Chung and Jahn, 1995; Chung et al., 1998; Wignall, 2001; Xu et al., 2001; Ali et al., 2002; Courtillot and Renne, 2002; Zhou et al., 2002; Lo et al., 2002). Although Chung and Jahn (1995) invoked the starting plume model to explain the outpouring of the Emeishan flood basalts, rigorous evaluation of the role of mantle plumes in the generation of this large igneous province was not available until recently (He et al., 2003; Xu et al., 2004; Zhang et al., 2006). Identification of mantle plumes in the Emeishan LIP is therefore not only important for deciphering the dynamic trigger of the Emeishan volcanism, but may be also relevant to the current debate surrounding the mantle plume theory.

This review paper summarizes some recent achievements made in studies of the Emeishan LIP. Eight aspects that are considered “diagnostic” of plume involvement will be evaluated here: (1) uplift prior to volcanism, (2) the chemical characteristics of the magma;

(3) high-temperature magma, (4) thermal zoning of the plume, (5) short duration of flood volcanism; (6) dimension and volume of magmas; (7) physical volcanology and (8) radiating dike swarm and age progression along hotspot tracks. Each section starts with a brief description of the theoretical basis for a particular prediction and/or criterion of mantle plumes, followed by presentation of respective observation and interpretation made in the Emeishan case. Data will be finally integrated to argue that the plume model remains a viable model to account for the generation of the Emeishan basalts.

Geological background

The Late Permian Emeishan basalts are erosional remnants of the voluminous mafic volcanic successions which occurred in the western margin of the Yangtze Craton, SW China. They are exposed in a rhombic area of 250 000 km^2 (Xu et al., 2001) bounded by the Longmenshan thrust fault in the northwest and the Ailaoshan-Red River (ASRR) slip fault in the southwest (Figure 1). However, some basalts and mafic complexes exposed in the Simao basin, northern Vietnam (west of the Ailaoshan fault), and in the Qiangtang terrain, Lijiang-Yanyuan belt and Songpan active fold belt (northwest of the Longmenshan fault) make possible an extension of the Emeishan LIP (Chung et al., 1998; Xiao et al., 2003, 2004a; Hanski et al., 2004). Some Emeishan-type basalts traced in southwest Yunnan and northern Vietnam may be related to the mid-Tertiary continental extrusion of Indochina relative to South China along the ASRR fault zone (Tapponnier et al., 1990; Chung et al., 1997). Three sub-provinces have been identified in the previous studies, namely the western, central and eastern parts of the Emeishan LIP (Figure 1, Cong, 1988; Zhang et al., 1988). The central part overlaps the "Panxi paleorift zone" (Tan, 1987). The thickness of the entire volcanic sequence in these sub-provinces varies considerably from over 5000 m in the west to a few hundred meters in the east. The province consists of dominant basaltic lavas and subordinate pyroclastic rocks. In the western sub-province, flows and tuff of trachytic and rhyolitic composition form an important part of the uppermost sequence (Huang, 1986; Chung et al., 1998; Xu et al., 2001). Such a compositional bimodality is also revealed by the associated intrusive rocks that comprise syenites and layered gabbros. Some syenites and gabbros are associated with massive V-Ti-Fe ore deposits (Sichuan, 1991; Yunnan, 1990).

The majority of the Emeishan basalts were sub-aerially erupted; only small portions are submarine facies and are restricted within the margin of the Emeishan LIP (Yunnan, 1990; He et al., 2006). The Emeishan volcanic successions unconformably overlie the late Middle Permian carbonate (i.e., the Maokou Formation) and are in turn covered by the uppermost Permian sedimentary rocks in the east and the Late Triassic sedimentary rocks in the central part of the Emeishan LIP (Figure 2a). The sedimentation in SW China, prior to the Emeishan flood volcanism, is characterized by a carbonate platform setting (Figure 3a; Wang et al., 1994; Feng et al., 1997). This carbonate platform consists of Liangshan (Lower Permian), Qixia and Maokou Formations (Middle Permian) (Figure 2a). The Middle and Upper Permian in the Upper Yangtze Craton is separated by an unconformity, referred to as the Dongwu unconformity. As a main constituent of the carbonate platform, the Maokou Formation, which immediately underlies the Emeishan basalts, is widespread in South China. It mainly consists of medium-bedded to massive limestones, with thickness ranging from 250 to 600 m. Abundant and rapidly evolved fossil assemblage permits division of the Maokou Formation into three biostratigraphic units, from bottom to top—the *Neoschwagerina simplex* zone, *Neoschwagerina craticulifera-Afghanella schencki* zone and *Yabeina-Neomisellina* zone (Figure 2a). These biostratigraphic units are well correlated throughout South China, thus making regional comparison/correlation possible.

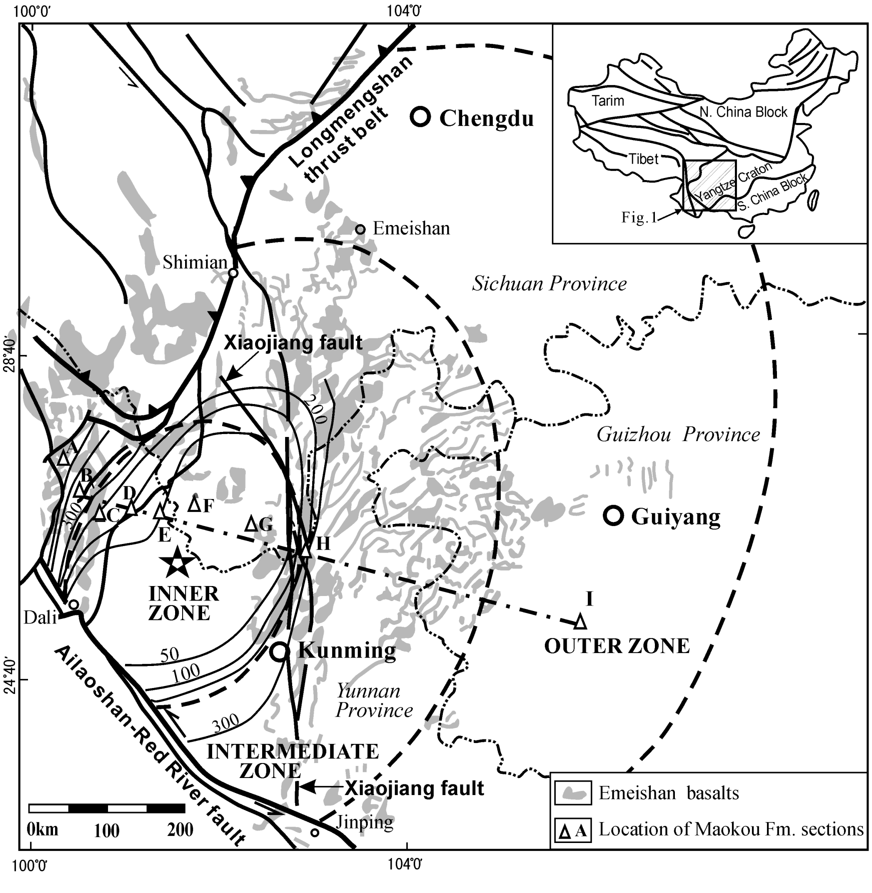

***Figure 1** Schematic map showing the distribution of the late Permian volcanic successions (grey areas) in the Emeishan large igenous province and adjacent regions (modified after Xu et al., 2004). The inset illustrates major tectonic unites in eastern Asia (after Chung et al., 1998). Also shown are isopachs of Maokou Formation that delineate a subcircular domal structure formed prior to Emeishan volcanism (He et al., 2003). Dashed curves separate inner, intermediate, and outer zones of dome, which are characterized by varying extent of erosion of Maokou limestone. Numbers indicate the thickness in meters.*

Pre-volcanic crustal uplift

Fluid dynamical and numerical modeling (Campbell and Griffiths, 1990; Griffiths and Campbell, 1991; Farnetani and Richards, 1994) suggest that when a mantle plume impinges on the lithosphere, the surface of the Earth should be elevated, producing roughly circular uplifts; the doming area may reach a diameter of 1000–2000 km, with 500–2000 m of relief depending on the viscosity and temperature of the plume head (Griffiths and Campbell, 1991). The plume theory also predicts that this uplift predates or takes place simultaneously with the volcanism. Pre-volcanic lithospheric uplift is ranked as the most fundamentally important criteria used to identify the presence of plumes (e.g., White and McKenzie 1989; Campbell and Griffiths, 1990; Campbell, 2001; Ernst and Buchan, 2001). Uplift is invariably best

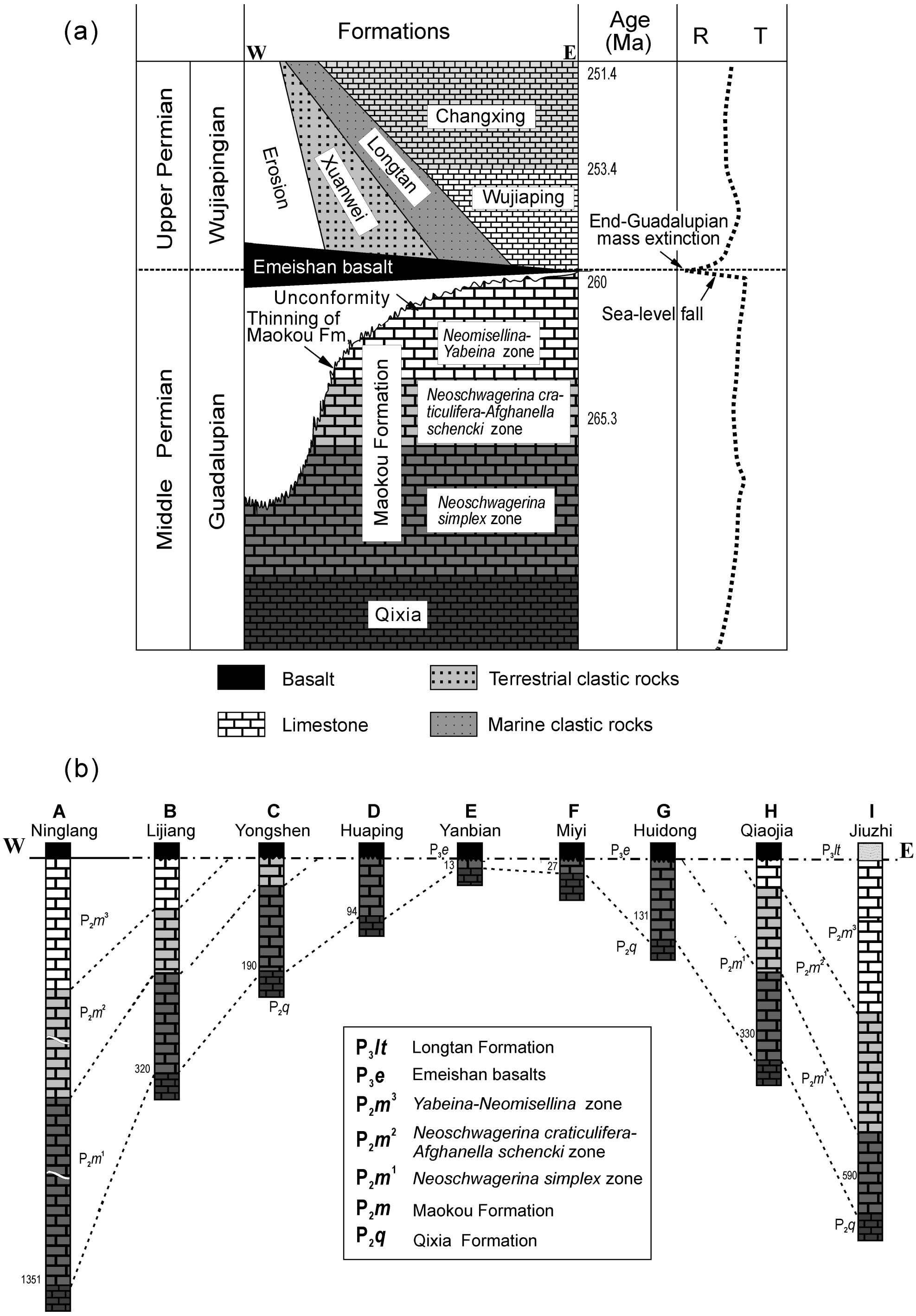

***Figure 2** (a) Generalized Permian stratigraphy and division of fusulinds zones in the western Guizhou Province (the outer zone of the Emeishan LIP) (modified after He et al., 2003; Xu et al., 2004). Age scheme is after Bowering et al. (1998) and Gradstein et al. (2004). Three biostratigraphic units comprise Maokou limestone. Curve assigning thinning of Maokou Formation (from west to east) is after He et al. (2003). Note that the Emeishan volcanism occurs at the upper and middle Permian boundary (see He et al., 2007). R—regression; T—transgression. (b) Biostratigraphic correlation of the Maokou Formation in the Emeishan LIP along west-east oriented traverse (the profile A–I in Figure 1) across the Emeishan LIP. Number near every section is the thickness of the Maokou Formation. Vertical scale is same for each section.*

recorded in the sedimentary record (Rainbird and Ernst, 2001) or in drainage patterns (Cox, 1989), such as localized shoaling, thinning of strata over the uplifted area, and erosional unconformity between the basalts and underlying sedimentary sequence (Rainbird and Ernst, 2001).

In order to characterize the crustal processes prior to the eruption of the Emeishan basalts, we examined the nature of the strata underneath the flood basalts (i.e., the Maokou Formation) and the contact between them, and compared paleogeography before and after the Emeishan volcanism. Systematic correlation and comparison of biostratigraphic units of the Maokou limestone reveal a domal thinning of the strata in the Emeishan LIP (Figure 2b). The thinned carbonates are capped by a subaerial unconformity, in many cases manifested by karst paleotopography, paleoweathering zone, and locally by relict gravels and basal conglomerates. Provenance analysis suggests that the gravels were mainly from the uppermost Maokou Formation. Therefore, the stratigraphic thinning likely resulted from differential erosion due to uplift. The isopach for the remnant Maokou limestone is not randomly distributed, but delineates a roughly sub-circular shape (Figure 1). This suggests that the erosion is most likely due to the pre-volcanic crustal uplift, which is broadly dome-shaped. He et al. (2003) estimated the extent of uplift >1000 m in the inner zone. The magnitude and shape of the uplift agree remarkably well with those predicted by Griffiths and Campbell (1991) and Farnetani and Richards (1994). The rapid uplift (less than a few million years) suggests that plume impact rather than plume incubation was responsible for the formation of the Emeishan LIP. The sedimentary records therefore provide independent supporting evidence for the starting plume initiation model for the generation of the Emeishan LIP.

In terms of the extent of erosion of the Maokou limestone, the Emeishan LIP can be divided into inner, intermediate and outer zones (Figure 1). The inner zone, where the Maokou Formation was strongly eroded, encloses west Yunnan and south Sichuan, and is about 400 km in diameter (Figure 1). The thickness of the Maokou Formation increases to 200–450 m in the intermediate zone and to 250–600 m in the outer zone (largely in Guizhou province). The apex of the uplift is likely coincident with the center of the postulated mantle plume. Accordingly, the center of the Emeishan plume is inferred to be located in the inner zone of erosion, i.e., at the central and partly western Emeishan LIP, an inference also reached by independent petrologic studies (Xu et al., 2001, 2004).

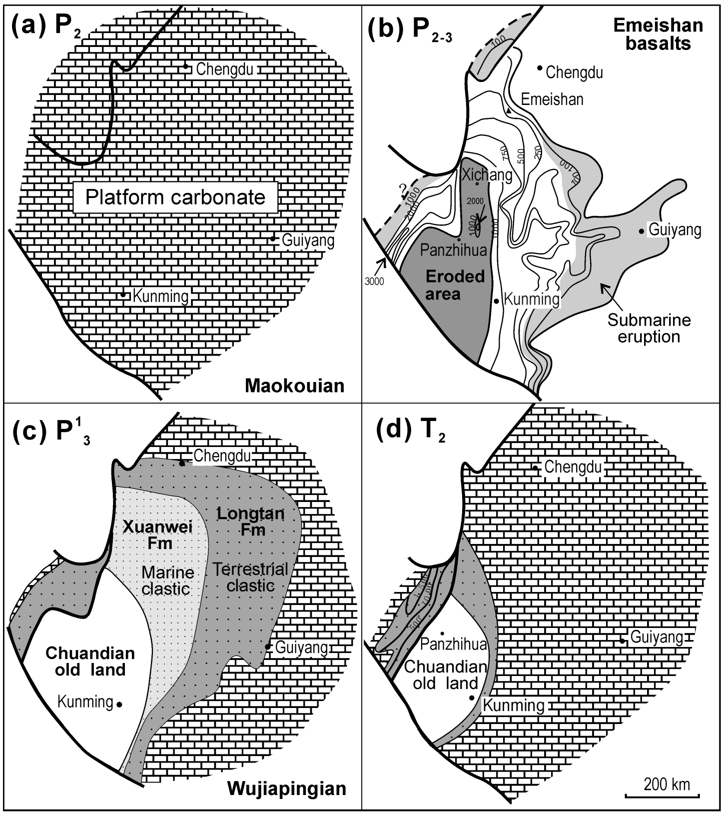

Figure 3 Diagram showing changes in sedimentation and lithofacies paleogeography before and after the Emeishan volcanism. (a) A stable, homogeneous carbonate platform in the Maokou stage (P_2), which is much bigger than the Emeishan LIP; (b) Isopach contours of remnant Emeishan basalt (P_{2-3}); (c) Paleogeography in the Wujiapingian ($P^1{}_3$); (d) Lithofacies paleogeography in the Middle Triassic (T_2). Data compiled from Feng et al. (1997), Wang et al. (1994).

As illustrated by the comparison of sedimentation before and after the Emeishan volcanism (Figure 3), plume uplift resulted in sub-aerial erosion of the carbonate platform to varying degrees in the late Middle Permian. Plume uplift also influences the geography of the western Yangtze Craton from late Permian to Middle Triassic (Figure 3). The distribution of the remnant Emeishan basalts appears to be dependent upon this domal structure (Figure 3b). The absence of the Emeishan basalts in the uplifted area (i.e., the inner zone) must have been due to enhanced erosion of this uplifted area. Figure 3c and Figure 3d also suggest a prolonged crustal uplift (~45 Myr) in the center of Emeishan LIP. This prolonged uplift cannot be due to plume impact on the base of the lithosphere, which is basically transient and would vanish after a short time due to decay of the thermal anomaly and/or deflation of the mantle head (Griffiths and Campbell, 1990; Farnetani et al., 1994). Instead, it is likely related to magmatic underplating (McKenzie, 1984; Cox, 1989; Brodie and White, 1994; Xu and He, in press).

Geochemistry

Overall, geochemical approach is not reliable in identifying ancient mantle plumes (Campbell, 2001) because of considerable overlaps in isotopic composition between modern plume-derived basalts and mid-ocean ridge basalts (MORB), and island arc basalts (IABs). The trace elements are more efficient for plume identification, but they are also affected by many factors (i.e., crustal contamination and lithospheric derivation) that can complicate the interpretation of trace elements in basalts. Nevertheless, uncontaminated plume-derived basalts should display geochemical signature resembling that of modern oceanic island basalts (OIB).

Classification of Emeishan basalts

The Emeishan flood basalts have been divided into two major magma-types—high-Ti (Ti/Y>500) and low-Ti (Ti/Y<500) basalts—on the basis of analyses of the samples from Binchuan and Ertan (Xu et al., 2001). The high-Ti group (HT) generally has higher Ti/Y (>500) and TiO_2 (>3.7 wt%) than the low-Ti ones (LT), which have low Ti/Y (<500) and TiO_2 (<2.5 wt%). This classification schema is confirmed by the large database obtained for the Binchuan and Jinping basalts (Xiao et al., 2003, 2004b). Moreover, available data permit a further subdivision of the low-Ti group into LT1 and LT2 types on the basis of trace element characteristics (Figure 4a–b). In general, the LT1 basalts have higher Mg# (67–61) than the LT2 basalts ($Mg^{\#}$ = 54–48) (Figure 4a). A more evolved nature is found for the HT basalts, for which $Mg^{\#}$ varies between 58 and 44. The distinction between the LT1 and LT2 lavas is also clear in the plotting of Th/Nb versus Ti/Y, which highlights the high contents of highly incompatible elements in the LT1 lavas (Figure 4b). LT1 lavas have higher Th/Nb (>0.17) ratios than the LT2 and HT basalts (Th/Nb <0.17). The measured and age-corrected $^{87}Sr/^{86}Sr$ and $^{143}Nd/^{144}Nd$ ratios of the Emeishan basalts define an array that lies near the "mantle correlation line", but is distinctly displaced to the right (Xu et al., 2001). In general, the HT basalts have relatively higher eNd(t) and lower $^{87}Sr/^{86}Sr(t)$ values than the LT basalts.

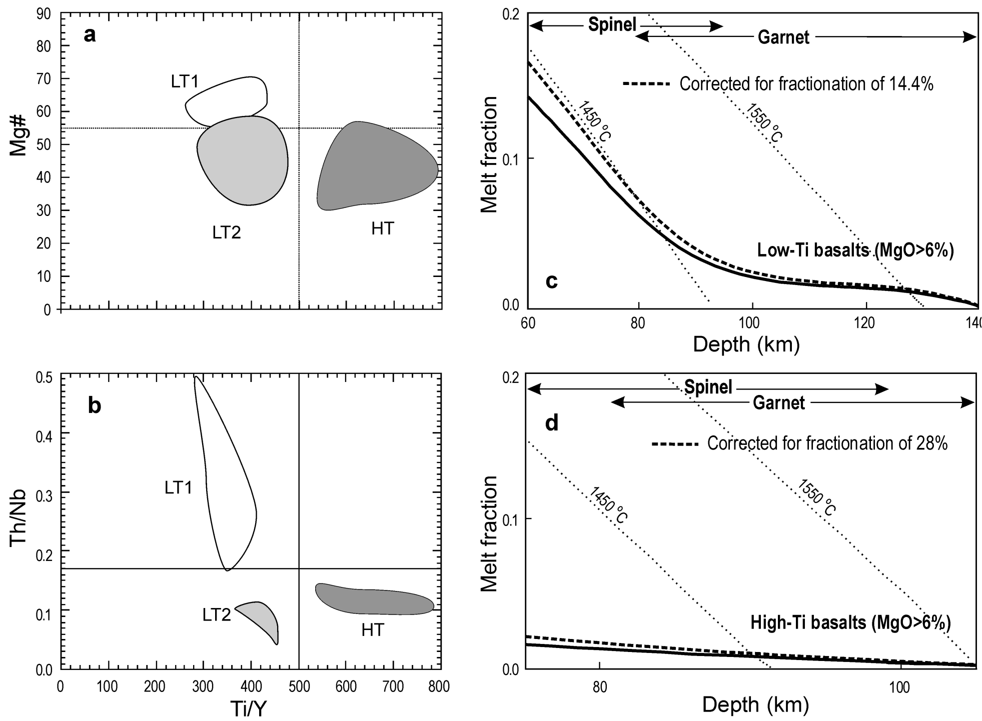

Figure 4 Classification of the Emeishan basalts in terms of Ti/Y versus Mg# (a) and Th/Nb (b). (c, d) Melt distribution for the Emeishan basalts (LT and HT) estimated from REE inversion (After Xu et al., 2001). Thin dashed line with labeled temperatures is the predicted melt distribution from isentropic decompression of mantle (White and McKenzie, 1995).

Melting conditions

Xu et al. (2001) adopted the fractional melting inversion of McKenzie and O'Nions (1991), incorporating the modification proposed by White et al. (1992), to quantitatively determine the melting conditions. The comparison between the melt distributions inferred from the LT lavas and the predicted one from mantle isentropic decompression indicates a mantle potential temperature of >1550 °C (Figure 4c). The melt distributions also show melting starting at a depth of 140 km. The upper limit of melting in the inversion is 60 km, typical of basalts generated beneath a stretched and thinned continental lithosphere. The maximum melt fraction estimated from inversion for LT lavas is about 16% (Figure 4c). In contrast, the maximum melt fraction estimated from inversion of the HT lavas is significantly low (1.5%; Figure 4d). The melting starts at ~100 km, and the upper limit of melting in the inversion is 75 km. These results suggest that the HT lavas were generated at a greater depth by a smaller degree of partial melting from mantle than the LT lavas. The potential temperature of the mantle involved in melt generation of the HT lavas is also relatively lower (<1500 °C) compared to that of the LT lavas.

Plume signature in the Emeishan basalts

The plume model for the Emeishan basalts is supported by compositional evidence, which is not equivocal for some important CFBs (e.g., Parana, Peate, 1997; Karoo, Ellam and Cox, 1991). Most HT and LT2 samples exhibit trace element ratios that overlap with the field of OIB. They show smooth trace element patterns that are very similar to OIB except for weak Nb anomaly in some samples (Figure 5). The pronounced negative Sr anomaly in HT lavas suggests that they have been affected by extensive fractionation of plagioclase. Samples with low trace element abundance also show high $\varepsilon_{Nd}(t)$ (4.6–4.8) and low $^{87}Sr/^{86}Sr(t)$ (0.7042–0.7046) values, thus likely reflecting the isotopic signature of the least-contaminated Emeishan plume head. A similar Sr-Nd isotopic composition of the plume head has also been proposed on the basis of analyses of the high-Ti/Y picritic lavas (Chung and Jahn, 1995). This indicates a depleted mantle source for the HT lavas, consistent with the relative depletion of Rb and Ba compared with Th, Ta and La in the HT samples (Figure 5).

Plume-lithosphere interaction

LT1 lavas show a negative Nb anomaly suggesting that components other than plume must have been involved in the generation and evolution of the Emeishan basalts. The most likely components are from the lithosphere (Figure 5c). There is still a hot debate about the way the lithosphere contributes to magma generation. Either lithospheric contamination of plume magmas by lithosphere-derived melts (Arndt et al., 1993) or wholescale melting of the subcontinental lithospheric mantle (CLM, Gallagher and Hawkesworth, 1992) has been proposed.

The chemical and isotopic composition of the LT samples may inherit that of the CLM (Xiao et al., 2004b). However, the thickness of the LT lavas in the Emeishan LIP is more than 3000 m. These lavas were emplaced during a relatively short time span (Huang and Opdyke, 1998; Lo et al., 2002; Ali et al., 2005; He et al., 2007). It is thus difficult to imagine that such a large volume of magma was generated by the melting of the lithospheric mantle, which is stable for a long time period in a non-convective state. The thermomechanical model suggests that only a small amount of melt can be produced from the lithospheric mantle by conduction of heat from the mantle plume (McKenzie and Bickle, 1988; Arndt and Christensen, 1992). The generation of the large amount of CFB is likely confined to the convective asthenosphere or plume. It has been argued that the melting temperature of the lithosphere may be considerably reduced by the presence of volatile phases, and the melting of hydrous CLM would more readily take place than that of the volatile-free plume (Gallagher and Hawkesworth, 1992). If this model applies to the Emeishan LIP, the LT lavas should be hydrous. However, primary biotites are only found in some HT lavas, and not in the LT samples (Xu et al., 2001). The geochemical variation of the LT1 lavas can therefore be accounted for by crustal contamination of plume-derived magmas. This is consistent with recent Os isotopic studies that suggest an insignificant role of the lithospheric mantle in the genesis of the Emeishan basalts (Suzuki et al., in press).

Contamination appears to have played a more important role in the LT lavas than in the HT lavas. The fact that LT1 lavas are overlain by LT2 and then HT lavas (Figure 6a) suggests that contamina-

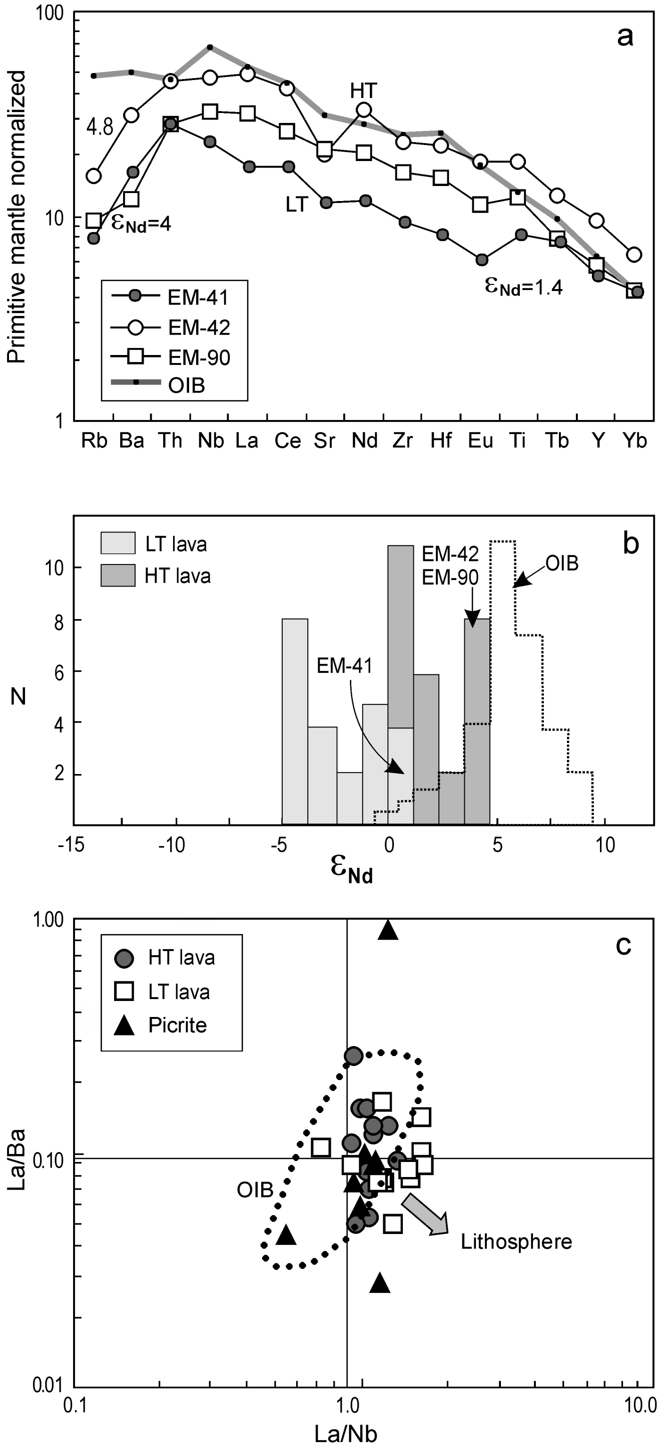

Figure 5 (a) Primitive mantle-normalized trace element concentrations of the uncontaminated basalts from Emeishan; (b) Comparison of isotopic composition of two series of basalts from Emeishan and OIB; (c) La/Ba versus La/Nb. Normalizing values are from Sun and McDonough (1989).

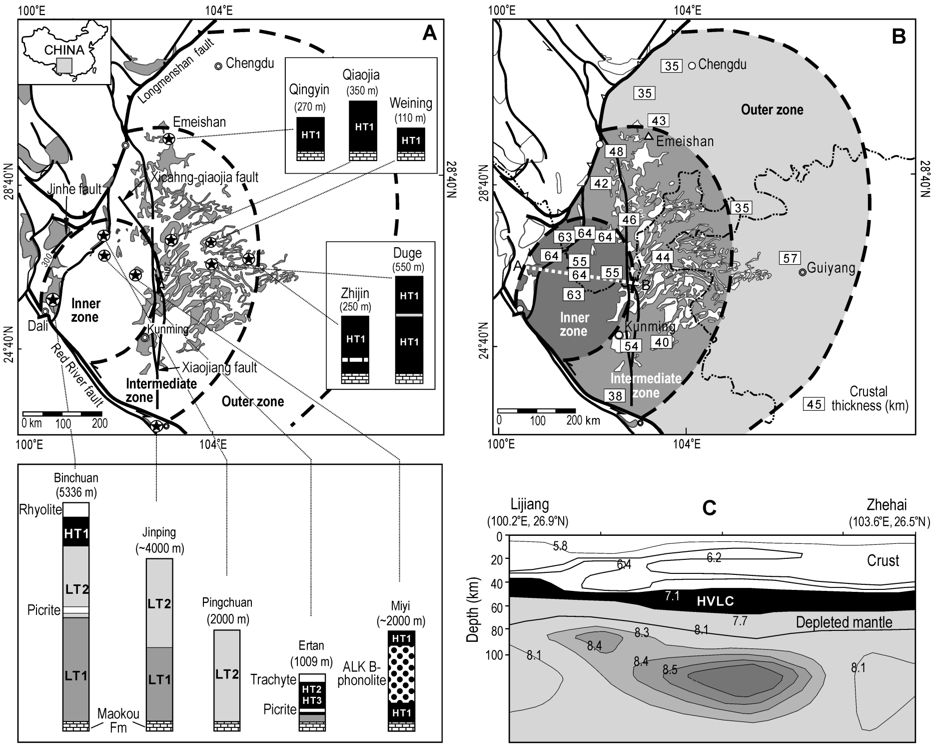

Figure 6 (a) Distribution of Late Permian Emeishan basalts in SW China and stratigraphic variation of 10 representative lava successions. HT—high-Ti basalt; LT—low-Ti basalt; ALK—alkaline series. Data sources: Xiao et al. (2003) and Xu et al. (2001, 2003, 2004). (b) Crustal thickness data plotted over domal area of Emeishan large igneous province. Data sources: Zhang et al. (1988), Yuan (1995), Liu et al. (2001). (c) Seismic velocity (Vp) structure of lower crust and upper mantle along profile A–B shown in (b) (modified from Liu et al., 2001). HVLC—high-velocity lower crust.

tion of plume-derived magma decreases with time. This could result from the decreasing assimilation of the wall-rock in conduit systems over time as successive eruptions gradually deplete available contamination material. The earlier magmas would be the most contaminated owing to disruption and erosion of wall rock during formation of the magmatic chamber. As these erupt and the conduits are coated with replenished fresh magmas, the degree of contamination tends to decrease. This is the likely scenario for the Emeishan LIP, because the least-contaminated LT lavas are located above the contaminated LT basalts, and evolved rhyolites at the top of the lava section typically have high $\varepsilon_{Nd}(t)$ (>2, Chung et al, unpublished data) (Xu et al., 2001).

Temperature

One of the major characteristics of mantle plumes is their excessive heat relative to the surrounding ambient asthenosphere. The magnitudes of thermal anomaly range up to 350°C (in the plume axis area, Farnetani and Richards, 1994) to ~100°C (in the margin of plume head, Campbell and Davies, 2006). Greater heat results in the plume mantle being less dense than normal, allowing it to rise to the base of the lithosphere. Large thermal anomaly within the mantle can explain the emplacement of the immense volume of magma over a rather short time span (Campbell and Griffiths, 1990). High-temperature mantle is also believed to be responsible for the occurrence of high magnesian rocks such as komatiites and picrites (Arndt and Nesbitt, 1982; Arndt, 2003).

Occurrence of picrites in the Emeishan LIP (Chung and Jahn, 1995; Zhang et al., 2006) provides first-order evidence for the thermal anomaly of the mantle from which the Emeishan basalts were derived. The potential temperature of a mantle can be estimated from the maximum MgO content of the erupted magmas, because the MgO content in magma increases with temperature (Takahashi et al., 1993). Since most flood basalts are fractionated, primary magma is the key to information about the mantle's temperature. The maximum MgO of the Emeishan picrites ranges from 16–21% (Chung and Jahn, 1995; Xu and Chung, 2001; Zhang et al., 2006), significantly higher than that of MORB (~12%). These maximum MgO contents suggest that the temperature excess for a mantle plume is between 100 and 250°C. Moreover, picrites exclusively occur in the inner zone, in agreement with the prediction that picrites should be most abundant near the center of the plume head and less abundant toward the margin (Campbell and Griffiths, 1990; Campbell and Davies, 2006).

Another way to estimate mantle potential temperature is the inversion model developed by McKenzie and O'Nions (1991), who use averaged REE concentrations of basalts to estimate the melt distribution as a function of depth, the total integrated melt fraction, and the total melt thickness, equivalent to the thickness of basaltic crust produced. The comparison between the melt distribution inferred from the LT lavas and the predicted one from isentropic decompression of the mantle (Figure 4c) indicates a potential mantle temperature of >1550°C (ΔT=~250°C).

The extent of the domal uplift can also be served as indicator of the mantle potential temperature, when it is compared to numerical modeling results. Fluid dynamical and numerical modeling suggests that the extent of pre-volcanic uplift is dependent on the viscosity of the plume head (Griffiths and Campbell, 1991). Specifically, with an excess temperature of 100°C, Griffiths and Campbell (1991) predicted an uplift of 500 m. A bigger uplift (2000 m) is obtained with an excess temperature of 350°C (Farnetani and Richards, 1994). The minimum uplift for the Emeishan LIP can be obtained from the depth of erosion of the underlying carbonate rocks (~500 m) in the inner and intermediate zones. He et al. (2003) obtained a higher estimate of ~1000 m, suggesting an excessive temperature in the order of ~200°C.

Spatial variation in basalt geochemistry and crustal structure

The plume hypothesis assumes that thermally anomalous materials arise from the core-mantle boundary. It predicts that the temperature of a plume should be highest at the plume axis, where the tail rises through the center of the head. The ΔT of the plume axis is expected to be ~300°C, compared to ~100°C at the rim of the plume head (Campbell and Davis, 2006). This thermally zoned structure of the plume head is responsible for spatial variation in lava thickness and crustal structure. For instance, in the North Altantic, crustal thickness ranges between 20 and 30 km at the plume axis, while it is 17–18 km at the margins of the head (Hopper et al., 2003).

The domal structure defined on the basis of paleogeography and sedimentation patterns provides a natural basis to subdividing the Emeishan LIP. This is important because the apex of the domed area may correspond to the plume head and the margins the plume head rims. Given the thermal gradient from the center to the rim of plume head, spatial variation in basalt chemistry is expected (Campbell and Griffiths, 1990). Xu et al. (2004) investigated compositional variations in the lavas from the center to the margin of the dome in the Emeishan LIP. Analyses of over 350 samples collected from ten vol-

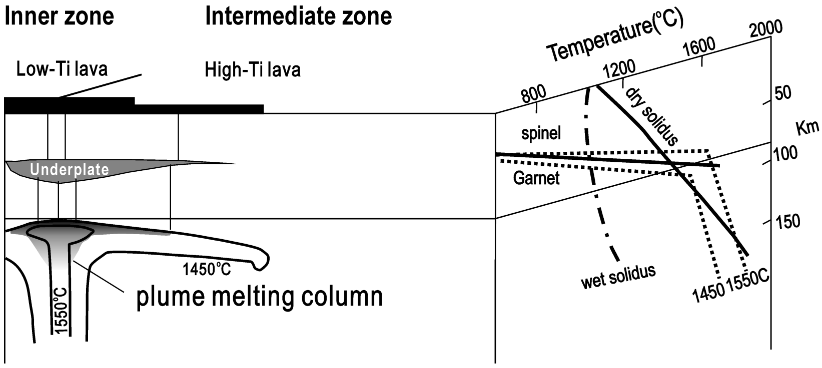

***Figure 7** Schematic diagram illustrating the thermal zonation of the Emeishan plume head that accounts for the spatial variation in lava composition/thickness and crustal thickness.*

cano-stratigraphic sections reveal a systematic change in basalt type from the inner to the intermediate zones (Figure 6). In general, the domed region of the Emeishan LIP comprises *thick* (2000–5000 m) sequences of low-Ti volcanic rocks and subordinate picrites (Chung and Jahn, 1995; Zhang et al., 2006). In contrast, *thin* sequences (<500 m) of high-Ti volcanic rocks mainly occur on the periphery of the domal structure (Figure 6). Since low-Ti samples may be derived by a higher degree of partial melting of the mantle at higher temperature than high-Ti samples (Figures, 4c,d; Xu et al., 2001), the transition from the low-Ti lavas in the inner zone to high-Ti lavas in the intermediate zone, is likely accompanied by a decreasing thermal gradient (Figure 7). This inference based on basalt geochemistry is remarkably consistent with that drawn from the sedimentary data.

The crust-mantle structure of the Emeishan LIP is apparently correlated with the domal structure as well. There is a gradual decrease in crustal thickness from the center to the margin of the dome (Figure 6b). Specifically, the thickness in the inner zone ranges from 55 to 64 km (av. 61.5 km) that is considerably thicker than in the intermediate zone (38–54 km, av. 45 km) (Yuan et al., 1995). The data in the outer zone defines a range of 35–43 km, typical of a non-rifted continental margin (Menzies et al., 2002). It is important to indicate that the thick crust in the inner zone consists of a high-velocity lower crust (HVLC, Vp = 7.1 to 7.8 km/s) with an average of 20 km (Figure 6c; Liu et al., 2001). The layer becomes gradually thinner toward the intermediate zone and is generally absent in the outer zone. This HVLC is interpreted as a result of magmatic underplating (Xu and He, in press). Consequently, a genetic link between crust-mantle structure and a mantle plume can thus be inferred. The thicker crust in the inner zone reflects high melt production resulting from higher temperature in the central part of the plume and uplift of lithosphere above the plume head which triggered relatively high amounts of decompression melting. Also high melt production may lead to cooling and fractionation of melts at the crust-mantle boundary thereby creating cumulate rocks that form the high-velocity lower crust (Farnetani et al., 1996). To sum up, the spatial variation in lava thickness and composition and in crustal thickness in the Emeishan LIP is consistent with the petrogenetic model indicating that melt production was higher in the inner zone (Figure 7).

Age and duration of flood basalt volcanism

Richards et al. (1989) pointed out that emplacement of immense volumes (of the order of 10^6 km^3) of basalt over a rather short time span (order of 1 Myr) is characteristic of large igneous provinces. Though remaining debated, short duration of volcanism is an important indicator of dynamic processes in depth, since it is believed that LIPs were the result of thermal mechanisms (Cordery et al., 1997; Farnetani and Richards, 1994; Farnetani et al., 1996).

An accurate determination of the age and duration of the Emeishan basalts is hindered because of the unsuccessful application of Ar-Ar radiometric dating technique to the Emeishan volcanic rocks. For instance, Boven et al. (2002) have performed $^{40}Ar/^{39}Ar$ dating on the lavas and intrusive rocks from the Emeishan LIP, but unfortunately they did not obtain plateau ages. It is suggested that the Emeishan basalts may have experienced a pervasive metamorphism probably during subsequent tectonization as a consequence of terrane amalgamation (Boven et al., 2002; Ali et al., 2004).

Lo et al. (2002) presented the first set of high-precision $^{40}Ar/^{39}Ar$ plateau ages of volcanic and intrusive rocks from the Emeishan traps. The results define a main stage of the flood magmatism at ~251–253 Ma (Table 1) and a subordinate precursory activity at ~255 Ma. This time span is generally coeval with, or slightly older than, the age of the Permian–Triassic boundary estimated from the ash beds in the Meishan stratotype section and the main eruption of the Siberian traps. However, these ages are not consistent with the stratigraphic relationship between the Emeishan basalts and Permian sedimentary rocks. The Emeishan basalts cover the Middle Permian Maokou Formation and are capped by the uppermost Permian Xuanwei Formation and Longtan Formation (equivalent to the Wujiaping Formation) in the eastern part of the province and by Triassic sediments in the central part. As discussed previously, the absence of the late Permian sequence in this area may be related to the uplifted topography compared to that in the western sub-province. The stratigraphic relationship therefore suggests that Emeishan basalts were erupted prior to the P-Tr boundary. Courtillot and Renne (2003) reviewed the ages of the major LIPs on Earth and put forward the hypothesis that most LIPs are emplaced in less than 1 Myr and

***Table 1** Summary of geochronological dating on diverse rocks of the Emeishan large igneous province.*

Geologic body	Dating method	Age (Ma)	Reference
Basalts in Binchuan section	Whole rock & mineral Ar-Ar	253-251 Ma	Lo et al. (2002)
Basalts from Guangxi	Whole rock Ar-Ar	254-256 Ma	Fan et al. (2004)
Subvolcanic rocks near Qiaojia	Whole rock Ar-Ar	258 Ma	Xu et al. (unpubl.).
Xinjie layered intrusion	Zircon SHRIMP U-Pb	259 ± 3 Ma	Zhou et al. (2002)
Panzhihua layered intrusion	Zircon SHRIMP U-Pb	263 ± 3 Ma	Zhou et al. (2005)
Mafic dyke in Devonian granite (Yanyuan)	Zircon SHRIMP U-Pb	262 ± 3 Ma	Guo et al. (2004)
Maomaogou syenite	Zircon SHRIMP U-Pb	261 ± 4 Ma	Luo et al. (2007)
Cida A-type granite	Zircon SHRIMP U-Pb	261 ± 4 Ma	Zhong et al. (2007)
Ailanghe I-type granite	Zircon SHRIMP U-Pb	251 ± 6 Ma	Zhong et al. (2007)
Silicic ignimbrite (Jiangwei)	Zircon SHRIMP U-Pb	263 ± 4 Ma	He et al. (2007)
Detrial zircons from the lowermost of Xuanwei Formation	Zircon SHRIMP U-Pb	257 ± 3 Ma	He et al. (2007)
Clay at the Upper-middle Permian boundary (Chaotian)	Zircon SHRIMP U-Pb	260 ± 4 Ma	He et al. (2007)

linked them with major bioclimatic events. Based on this hypothesis, Courtillot et al. (1999) predicted that the Emeishan LIP was emplaced at the end Guadalupian (~258 Ma). However, the stratigraphic constraint on the termination of Emeishan volcanism remains unclear, because it is not certain whether the Xuanwei Formation is a lateral equivalent of the Wuchiapingian or the Luopingian.

Recent Ar-Ar radiometric dating on Permian basalts exposed in western Guangxi (Fan et al., 2004) and subvolcanic rocks near Qiaojia (Xu et al., unpublished data) yield 254–256 Ma and 258 Ma, respectively. These estimates are more or less consistent with the stratigraphic constraints, strongly suggesting that the emplacement of the Emeishan basalts took place prior to the Permian–Triassic boundary. More meaningful ages come from the Sensitive High-Resolution Ion Microprobe (SHRIMP) zircon U-Pb age determination (Table 1), which yield systematically older ages than Ar-Ar techniques. Petrogenetic assessment suggests that the sediments in the Xuanwei Formation were derived from the erosion of the Emeishan volcanic rocks in the inner zone (He et al., 2007). In particular, the sediments in the lowermost of the Xuanwei Formation mainly represent eroded materials of the silicic member of the uppermost sequence of the Emeishan volcanic succession. Therefore the base of the Xuanwei Formation provides a firm limit on the termination of the Emeishan volcanism. Moreover, the Chaotian clay bed (Northern Sichuan) at the middle-late Permian boundary has been demonstrated to be genetically related to the Emeishan silicic volcanism (Isozaki et al., 2004). Given the fact that both the Emeishan basalt and the Chaotian clay rest on the Maokou Formation, the Emeishan basalt is inferred to be the stratigraphic equivalent of the clay bed at the Chaotian section (He et al., 2007). It follows that the main phase of the Emeishan volcanism must have been emplaced *prior to* the Wuchiapingian stage and most likely occurred at the Middle-Late Permian boundary (Figure 2).

The suggestion that the Emeishan volcanism is a boundary event yields important implications for the age and duration of this large igneous province. Specifically, the age of the Middle-Late Permian boundary (260.4±0.4 Ma, Gradstein et al., 2004) can be taken as the timing of the main phase of the Emeishan flood volcanism. This inference is confirmed by recent U-Pb analyses on zircons from the mafic and alkaline intrusions (Table 1; Zhou et al., 2002, 2005; Zhong et al., 2006, 2007; Luo et al., in press; He et al., 2007), assuming that these layer intrusions are feeding dykes of volcanism. For instance, using SHRIMP to analyze zircons, Zhou et al. (2002) established the age of the Xinjie intrusion in the Emeishan igneous province at 259±3 Ma.

Geochronologic data of the lowermost Xuanwei Formation, in which the zircons inherited felsic extrusives in the uppermost Emeishan lava sequences, place constraints on the absolute termination age of the Emeishan volcanism. SHRIMP analyses on two samples yield 257±3 Ma and 260±5 Ma. Despite the relatively large uncertainty, which could be due to the nature of the zircons in these samples, these ages are indistinguishable within error from the Middle-Late Permian boundary age (260.4±0.4 Ma; Gradtein et al., 2004), and are also very close to the age of the main phase of volcanism (e.g., 259±3 Ma; Zhou et al., 2002). Consequently, a very short duration (a few Ma) may be inferred for the Emeishan volcanism. Previous arguments for a short duration of the Emeishan volcanism had been mainly based on the consideration of weathered features (Xu et al., 2001) and comparison of paleomagnetic data from a section in the east of the province with the perceived magnetostratigraphy of the period (Huang and Opdyke, 1998). Huang and Opdyke (1998) studied a 550-m-thick, 12-unit Emeishan basalt section at Duge, Guizhou Province (~170 km west of Guiyang). A normal-polarity magnetozone was identified in the lower 6 units (spanning 449 m of section). An overlying reverse-polarity magnetozone was recorded in Units 8–12 (449–551 m). This suggested that the Emeishan basalts were mainly erupted in one normal-polarity episode, thereby implying rapid emplacement. A similar conclusion was reached by Ali et al. (2002), who noted that almost all of the sample-site polarities reported in the tectonically orientated palaeomagnetism studies were "normal".

Volume and areal extent of Emeishan basalts

Plume materials arise because they are warmer and lighter than the overlying mantle. But the plume has to gather enough buoyancy to overcome the viscosity of the mantle that opposes its rise (Griffiths and Campbell, 1990; Campbell, 2005). Consequently, new plumes have a large head followed by a relatively small tail. Plume tails have a high temperature. When a plume head reaches the top of its ascent, it flattens to form a disk with diameter twice that of the head. The length of a typical plume head can reach as much as 2000 km. The plume head can produce millions of cubic km of magma (Campbell and Davies, 2006). Modeling of melting in a mantle plume head by Leith and Davis (2001) typically yields melting rates of 1–10 km^3/a and a total melt volume of 1–20 million km^3. These results cover the range of observed melting rates and volumes of most LIPs. For instance, the Siberian traps extent over an area of 10^6 km^2. The area extent agrees well with the dimension of the plume head. Hence, the huge volume and vast dimension of igneous province can be taken as a viable criterion for identifying ancient mantle plume.

Some doubts have been cast on the viability of the plume model in the Emeishan case because of its relatively small dimension compared with typical LIPs (e.g., Thompson et al., 2001). Lin (1985) estimated the average lava thickness of the Emeishan basalt to be about 700 m. Taking the exposure surface of 2.5×10^5 km^2, the entire volume of the Emeishan basalt is estimated to be $\sim0.2\times10^6$ km^3. This must represent a minimum estimate (Xu et al., 2001) because: (1) complicated tectonic movements in Meso-Cenozoic eras in this region cut off the western extension of the LIP (Chung et al., 1998, Xiao et al., 2003); (2) erosion must have removed a significant portion of the eruptive sequences (He et al., 2006); and (3) the associated intrusives are not taken into account. Specifically, the Emeishan LIP was traditionally thought to be bounded by the ASRR fault in the southwest (Figure 1). However, the pre-Cretaceous strata in the Jinping area, located in the southwest of the ASRR fault, are comparable with those in the Binchuan area within the western margin of the Emeishan LIP. This stratigraphic correlation is reinforced by the similar chemo-stratigraphic variation of the late Permian basalts from the two spatially separated regions (Xiao et al., 2003). Therefore, the Jinping basalts, which crop out ~500 km southeast of the Binchuan counterpart, are identified as a dismembered part of the Emeishan basalts that were displaced to the present location by the mid-Tertiary sinistral movement along the ASRR fault. This correlation, together with the Emeishan-type basalts in northern Vietnam (Hanski et al., 2004) and in the Garz-Litang region (Xiao et al., 2004a), allows us to suggest that the ASRR fault does not bound the Emeishan LIP. Thus, this LIP has a much larger extent, and its western boundary was likely located in the Paleo-Tethyan ocean, which was closed during the Triassic.

The emplacement of igneous materials in the lower crust was genetically related to the erupted basalts (Xu et al., 2004; Xu and He, 2007); therefore, this high velocity layer can be considered as an integral part of the Emeishan LIP. The HVLC likely occurs predominantly within the inner zone of the dome, given the contrast in the crust-mantle structure between the inner zone and other zones. In this sense, a minimum volume (2.5×10^6 km^3) of igneous materials accreted to pre-existing crust can be estimated. A higher estimate could be expected if intraplating (i.e., magmas trapped at different crustal level) is taken into account. This estimate in turn provides constraints on the volume of erupted lavas, as cumulates and erupted magmas can be related by mass balance (Cox, 1989):

$$C_P = C_L X_L + C_C X_C$$

where C_P, C_L, and C_C are the concentrations of an element in parental magma, erupted liquid and cumulate respectively; X_L and X_C are the respective mass fractions of erupted liquid and cumulates. Using the above equation and elemental concentrations in parents, erupted basalts and cumulate, the ratio X_C/X_L of 0.65 is obtained. Accordingly, the minimum volume of erupted magmas is estimated at 3.8×10^6 km^3, equivalent to the volume of the Earth's typical large igneous provinces (Coffin and Eldholm, 1994). As a consequence, the volume of igneous materials is not at odds with the plume model proposed for the formation of the Emeishan LIP.

Physical volcanology

Most of the plume-derived basalts that have been preserved in the geologic record are continental volcanic sequences (Campbell, 2001). Subaerial eruption in a continental setting makes the eruptive style and physical volcanology of continental flood basalts significantly different from those for MORB and IAB, because the latter are mostly below sea-level. On the other hand, due to the relatively low temperature and volatile-rich nature, pyroclastic deposits dominate the main eruptive phase of subduction-related volcanism. Furthermore, subduction-related lavas do not flow over large distances because of high viscosity. In contrast, plume-derived magmas are characterized by high temperature and low viscosity. As such, flood basalt flows spread over large distances, making large-scale stratigraphic correlation possible. Because of low volatile content in flood basalts, pyroclastic rocks are rare in CFB. Physical volcanology suggests that the Emeishan basalts were mainly erupted under subareal conditions. Volcanism is composed of dominant lava flows and only subordinate pyroclastic deposits. Such features resemble those typical of plume-derived basalts.

Dike swarms and age progression along volcanic chain

Radiating dike swarms, especially giant dike swarms with lengths >300 km, are an important tool for identifying and locating mantle plumes. These radiating dike swarms are thought to converge at the centres of arriving plume heads (Ernst et al., 1995; Ernst and Buchan, 2001). Typical examples include Proterozoic Mackenzie dyke swarms. Investigation into the plume-related dyke in the Emeishan case is limited; field mapping and precise dating are required in future studies.

Hotspot tracks are commonly observed in oceanic settings. Chains of volcanoes are produced when a relatively thin oceanic lithosphere passes through stationary strong plume tails (Wilson, 1967). However, similar chains of volcanoes are rare on continental crust. This is largely because the thick continental lithosphere arrests the ascent of the mantle plume at greater depth. Consequently, plumes undergo lower degrees of partial melting, forming widely spaced volcanoes rather than volcanic chains. The same reason can explain the lack of volcanic chains in the Emeishan LIP.

Summary and conclusions

The most convincing arguments in support of an ancient plume include pre-volcanic crustal uplift, high-temperature magmas, thermal zoning structure, geochemistry, duration of volcanism, extent and volume of volcanism, physical volcanology, hotspot tracks and radiating dyke swarm. Data summarized in this review suggest that the Emeishan LIP meets 7 out of the 9 criteria. In particular, sedimentologic and paleogeographic data show unequivocal evidence of a lithospheric doming event prior to the Emeishan volcanism. In turn this analysis provides a unique framework within which data from many disciplines can be consistently interpreted in terms of the mantle plume hypothesis. The data obtained in the Emeishan LIP are therefore in strong support of the existence of mantle plumes.

Acknowledgements

The study benefited from financial supports by the National Natural Science Foundation of China (40421303; 40234046) and the Chinese Academy of Sciences (KZCX2-101, the Bairen project).

References

Ali, J.R., Thompson, G.M., Song, X., and Wang, Y. 2002, Emeishan Basalts (SW China) and the "end-Guadalupian" crisis: magnetobiostratigraphic constraints: Journal of Geological Society (London), v. 159, pp. 21–29.

Ali, J.R., Thompson, G.M., Zhou, M.F., and Song, X.Y., 2004, Emeishan Basalts Ar-Ar overprint ages define several tectonic events that affected the western Yangtze Platform in the Meso- and Cenozoic: Journal of Asian Earth Sciences, v. 23, pp. 163–178.

Ali, J.R., Thompson, G.M., Zhou, M.F., and Song, X.Y. 2005, Emeishan large igneous province, SW China: Lithos, v. 79, pp. 475–489.

Anderson, D.L., 2000, The thermal state of the upper mantle: No role for mantle plumes: Geophysical Research Letter, v. 27, pp. 3623–3626.

Arndt, N.T., 2003, Komatiites, kimberlites, and boninites: Journal of Geophysical Research, v. 108, pp. 2293, doi: 10.1029/2002JB002157.

Arndt, N.T. and Christensen, U., 1992, The role of lithospheric mantle in continental flood volcanism: thermal and geochemical constraints: Journal of Geophysical Research, v. 97, pp. 10967–10981.

Arndt, N.T. and Nesbitt, R.W., 1982, Geochemistry of Munro Township basalts, in Komatiites: Allen and Unwin, Concord, Mass, pp. 309–330.

Besse, J. and Courtillot, V.E., 2002, Apparent and true polar wander and the geometry of the geomagnetic field over the last 200 Myr: Journal of Geophysical Research, v. 107, doi: 10.1029/2000JB000050.

Boven, A., Pasteels, P., Punzalan, L.E., Liu, J., Luo, X., Zhang, W., Guo, Z., and Hertogen, J., 2002, $^{40}Ar/^{39}Ar$ geochronological constraints on the age and evolution of Permo-Triassic Emeishan volcanic province, Southwest China: Journal of Asian Earth Sciences, v. 20, pp. 157–175.

Brodie, J. and White, N., 1994, Sedimentary basin inversion caused by igneous underplating: Northwest European continental shelf: Geology. V. 22, pp. 147–150.

Campbell, I.H., 2001. Identification of ancient mantle plumes, *in* Ernst R.E. and Buchan, ed., Mantle plumes: their identification through time: Geological Society of America Special Papers, v. 352, pp. 5–22.

Campbell, I.H., 2005, Large igneous provinces and the mantle plume hypothesis: Element, v. 1, pp. 265–269.

Campbell, I.H. and Davies, G.F., 2006, Do mantle plumes exist? Episodes, v. 29, pp. 162–168.

Campbell, I.H. and Griffiths, R.W., 1990, Implications of mantle plume structure for the evolution of flood basalts: Earth and Planetary Science Letters, v. 99, pp. 79–93.

Chung, S.L. and Jahn, B.M., 1995, Plume-lithosphere interaction in generation of the Emeishan flood basalts at the Permian-Triassic boundary: Geology, v. 23, pp. 889–892.

Chung, S.L., Jahn, B.M., Wu, G.Y., Lo, C.H., and Cong, B.L., 1998, The Emeishan flood basalt in SW China: a mantle plume initiation model and its connection with continental break-up and mass extinction at the Permian-Triassic boundary, *in* Flower, M.F.J., Chung, S.L., Lo, C.H. and Lee, T.Y. (eds.), Mantle Dynamics and Plate Interaction in East Asia. AGU Geodynamic Series, v. 27, pp. 47–58.

Chung, S.L., Lee, T.Y., Lo, C.H., Wang, P.L., Chen, C.Y., Nguyen, T.Y., Tran, T.H., and Wu, G.Y., 1997, Intraplate extension prior to continental extrusion along the Ailao Shan–Red River shear zone: Geology, v. 25, pp. 311–314.

Christiansen, R.L., Foulger, G.R., and Evans. J.R., 2002, Upper mantle origin of the Yellowstone hotspot: Bulletin of Geological Society of America. v. 114, pp. 1245–1256.

Coffin, M.F. and Eldholm, O., 1994, Large igneous provinces: crustal structure, dimensions, and external consequences: Review of Geophysics, v. 32, pp. 1–36.

Cong, B., 1988, The formation and evolution of the Panxi paleo-rift system: Scientific publishing house (in Chinese).

Cordery, M.J., Davies, G.F., and Campbell, I.H., 1997, Genesis of flood basalts from eclogite-bearing mantle plumes: Journal of Geophysical Research, v. 102, pp. 20,179–20,220.

Courtillot, V., Davaillie, A., Besse, J., and Stock, J., 2003, Three distinct types of hotspots in the Earth's mantle: Earth and Planetary Science Letters, v. 205, pp. 295–308.

Courtillot, V., Jaupart, C., and Manighetti, I., 1999, On causal links between flood basalts and continental breakup: Earth and Planetary Science Letters, v. 166, pp. 177–195.

Courtillot, V.E. and Renne, P.R., 2003, On the age of flood basalt events: Geoscience, v. 335, pp. 113–140.

Cox, K.G., 1989, The role of mantle plumes in the development of continental drainage patterns: Nature, v. 342, pp. 873–877.

DePaolo, D. and Manga, M., 2003, Deep origin of hotspots – Is only seeing believing?: Science, v. 300, pp. 920–921.

Ellam, R.M. and Cox, K., 1991, An interpretation of Karoo picrite basalts in terms of interaction between asthenospheric magmas and the mantle lithosphere: Earth and Planetary Science Letters, v. 105, pp. 330–342.

Ernst, R.E. and Buchan, K., 2001, Mantle plumes: their identification through time: Geological Society of America Special Papers.

Ernst, R.E., Head, J.W., Parfitt, E., Crosfils, E., and Wilson, L., 1995, Giant radiating dyke swarms on Earth and Venus: Earth-Science Reviews, v. 39, pp. 1–59

Fan, W.M., Wang, Y.J., Peng, T.P., Miao, L.C., and Guo, F., 2004, Ar-Ar and U-Pb chronology of late Palaozoic basalts in western Guangxi and its constraints on the eruption age of the Emeishan basalt magmatism: Chinese Science Bulletin, v. 49, pp. 2318–2327.

Farnetani, C.G. and Richards, M.A., 1994, Numerical investigation of the mantle plume initiation model for flood basalt event: Journal of Geophysical Research, v. 99, pp. 13813–13883.

Farnetani, C.G., Richards, M.A., and Ghiorso, M.S., 1996, Petrological models of magma evolution and deep crustal structure beneath hotspots and flood basalts: Earth and Planetary Science Letters, v. 143, pp. 81–94.

Feng, Z.Z.; Yang, Y.Q., and Jin, Z.K., 1997, Lithofacies paleography of Permian of south China: Beijing Petroleum University Press. 242p. (in Chinese with English abstract).

Foulger, G.R., 2002, Plumes, or plate tectonic processes?: Astronomy and Geophysics, v. 43, pp. 6.19–6.23.

Foulger, G.R. and Natland, J.H., 2003, Is "hotspot" volcanism a consequence of plate tectonics?: Science, v. 300, pp. 921–922.

Foulger, G.R., Pritchard, M.J., Julian, B.R., Evans, J.R., Allen, R.M., Nolet, G., Morgen, W.J., Bergsson, B.H., Erlendsson, P., Jakobsdottir, S., Ragnarsson, Stefanssoln, R., and Vogfjord, K., 2000, The seismic anomaly beneath Iceland extends down to the mantle transition zone and no deeper. Geophysical Journal International, v. 142, pp. F1–F5.

Gallagher, K. and Hawkesworth, C.J., 1992, Dehydration melting and the generation of continental flood basalts: Nature, v. 358, pp. 57–59.

Gradstein, F.M., Ogg, J.G., Smith, A.G., Bleeker, W., and Lourens, L.J., 2004, A new geologic time scale, with special reference to Precambrian and Neogene: Episodes, v. 22, pp. 83–99.

Griffiths, R.W. and Campbell, I.H., 1990, Stirring and structure in mantle starting plumes: Earth and Planetary Science Letters, v. 99, pp. 66–78.

Griffiths, R.W. and Campbell, I.H., 1991, Interaction of mantle plume heads with the Earth's surface and onset small-scale convection: Journal of Geophysical Research, v. 96, pp. 18275–18310.

Guo, F., Fan, W.M., Wang, Y.J., and Li, C.W., 2004, When did the Emeishan plume activity start? Geochronological evidence from ultramafic-mafic dikes in Southwestern China: International Geology Review, v. 46, pp. 226–234.

Hanski, E., Walker, R.J., Huhma, H., Polyakov, G.V., Balykin, Hoa T.T., and Phuong, N.T., 2004, Origin of the Permian-Triassic komatiites, northwestern Vietnam: Contributions to Mineralogy and Petrology, v. 147, pp. 453–469.

He, B., Xu, Y.-G., Chung, S.-L., Xiao, L., and Wang, Y., 2003, Sedimentary evidence for a rapid crustal doming prior to the eruption of the Emeishan flood basalts: Earth and Planetary Science Letters, v. 213, pp. 389–403.

He, B., Xu, Y.G., Huang, X.L., Luo, Z.Y., Shi , Y.R., Yang, Q.J., and Yu, S.Y., 2007, Age and duration of the Emeishan flood volcanism, SW China: Geochemistry and SHRIMP zircon U-Pb dating of silicic ignimbrites, post-volcanic Xuanwei Formation and clay tuff at the Chaotian section: Earth and Planetary Science Letters (in press).

He, B., Xu, Y.G., Wang , Y.M., and Luo, Z.Y., 2006, Sedimentation and lithofacies paleogeography in SW China before and after the Emeishan flood volcanism: New insights into surface response to mantle plume activity: Journal of Geology, v. 114, pp. 117–132.

Hopper, J.R., Dahl-Jensen, T., Holbrook, W.S., Larson, H.C., Lizarralde, D., Korenaga, J. Kent, G.M., and Kelemen, P.B., 2003, Structure of the SE Greenland margin from seismic reflection and refraction data: implications for nascent spreading center subsidence and asymmetric crustal accretion during North Atlantic opening: Journal of Geophysical Research, v. 108, 2269: doi: 10.1029/2002.JB001996.

Huang, K.N., 1986, The petrological and geochemical characteristics of the Emeishan basalts from SW China and the tectonic setting of their formation (Ph.D. thesis): Institute of Geology, Academy Sinica (in Chinese).

Huang, K.N. and Opdyke, N.D., 1998, Magnetostratigraphic investigations on an Emeishan basalt section in western Guizhou province, China: Earth and Planetary Science Letters, v. 163, pp. 1–14.

Isozaki, Y., Yao, J.X., Matsuda, T., Sakai, H., Ji, Z.S., Shimizu, N., Kobayashi, N., Kawahata, H., Nishi, H., Takano, M., and Kubo, T., 2004. Stratigraphy of the Middle-Upper Permian and Lower Triassic at Chaotian, Sichuan, China: Proceedings of Japan Academy, v. 80, ser. B, pp. 10–16.

Kerr, A.C., England, R.W., and Wignall, P.B., 2005, Mantle plumes: physical processes, chemical signatures, biological effects: Lithos, v. 79, pp. vii–x.

Leith, A.M. and Davis, G.F., 2001, Mantle plumes from flood basalts: enhanced melting from plume ascent and an eclogite component: Journal of Geophysical Research, v. 106, pp. 2047–2059.

Lin, J.Y., 1985, Spatial and temporal distribution of Emeishan basaltic rocks in three southwestern province (Sichuan, Yunnan and Guizhou) of China: Chinese Science Bulletin, v. 12, pp. 929–932 (in Chinese)

Liu, J.H., Liu, F.T., He, J.K., Chen, H., and You, Q.Y., 2001, Study of seismic tomography in Panxi paleorift area of southwestern China—structural features of crust and mantle and their evolution: Science in China (Series D), v. 44, pp. 277–288.

Lo, C.H., Chung, S.L., Lee, T.Y., and Wu, G.Y., 2002, Age of the Emeishan flood magmatism and relations to Permian-Triassic boundary events: Earth and Planetary Science Letters, v. 198, pp. 449–458.

Luo, Z.Y., Xu, Y.G., He B., Shi Y.R., and Huang, X.L., 2007, Geochronologic and petrochemical evidence for the genetic link between the Maomaogou nepheline syenites and the Emeishan large igneous province: Chinese Science Bulletin (in press).

McKenzie, D., 1984, A possible mechanism for epeirogenic uplift: Nature. v. 307, pp. 616–618.

McKenzie, D.P. and Bickle, M.J., 1988, The volume and composition of melt generated by extension of the lithosphere: Journal of Petrology, v. 29, pp. 625–679.

McKenzie, D.P. and O'Nions, R.K., 1991, Partial melt distributions from inversion of rare earth element concentrations: Journal of Petrology, v. 32, pp. 1021–1091.

Menzies, M.A., Klemperer, S.L., Ebinger, C.J., and Baker, J., 2002, Characteristics of volcanic rifted margins, *in* Menzies, M.A., et al., eds., Volcanic rifted margins: Geological Society of America Special Paper, v.362, pp.1–14.

Montelli, R., Nolet, G., and Dahlen, F.A., 2004, Finite-frequency tomography reveals a variety of plumes in the mantle: Science, v. 303, pp. 338–343.

Morgan, W.J., 1971, Convection plumes in the lower mantle, Nature, v. 230, pp. 42–43.

Peate, D.W., 1997, The Parana-Etendeka Province, *in* Mathoney, J. and Coffin, B. (eds), Large igneous provinces: continental, oceanic and planetary flood volcanism: AGU Geophysical Monograph, v. 100, pp. 217–246.

Rainbird, R.H. and Ernst, R.E., 2001, The sedimentary record of mantle-plume uplift, *in* Ernst, R.E. and Buchan, K.L., eds., Mantle plumes: their identification through time: Boulder, Colorado: Geological Society of America Special Paper, v. 352, pp. 227–245.

Renne, P.R., Zhang, Z.C., Richards, M.A., Black, E., and Basu, A.R., 1995, Synchrony and causal relations between Permian-Triassic boundary crises and Siberian flood volcanism: Science, v. 269, pp. 1413–1416.

Richards, M.A., Duncan, R.A. and Courtillot, V.E., 1989, Flood basalts and hotspot tracks: plume heads and tails: Science, v. 246, pp. 103–107.

Sichuan (Anonymous), 1991, Regional geology of Sichuan province: Geological Memoir Series 23, Geological Publishing House, Beijing, 730 pp (in Chinese).

Steinberger, B. Sutherland, R. and O'Connell R.J., 2004, Prediction of Emperor-Hawaii seamount locations from a revised model of global plate motion and mantle flow: Nature, v. 430, pp. 167–173.

Stolper, E., 1980. A phase diagram for mid-ocean ridge basalts: preliminary results and implications for petrogenesis: Contributions to Mineralogy and Petrology, v. 74, pp. 13–27.

Sun, S.-S. and McDonough, W.F., 1989. Chemical and isotopic systematics of oceanic basalts: implications for mantle composition and processes, *in* Saunders, A.D. and Norry, M.J. (eds), Magmatism in the Ocean Basins: Geol. Soc. London Special Publication, v. 42, pp. 313–345.

Takahashi, E., Shimazaki, T. and Tsuzaki, Y., 1993. Melting study of a peridotite KLB-1 to 6.5 GPa, and the origin of basaltic magmas. Phil Trans R Soc London, v. A342, pp. 105–120.

Tan, T.K., 1987, Geodynamics and tectonic evolution of the Panxi rift: Tectonophysics, v. 133, pp. 287–304.

Tarduno, J.A., Duncan R.A., Scholl, D.W., Cottrell, R.D., Steinberger, B., Thordarson, T., Kerr, B.C., Neal, C.R., Frey, F.A., Torii, M., and Carvallo, C., 2003, The Emperor seamounts: southward motion of the Hawaiian hotspot plume in the Earth's mantle: Science, v.301, pp. 1064–1069.

Tapponnier, P., Lacassin, R., Leloup, P.H., Scharer, U., Zhong, D.L., Wu, H.W., Liu, X.H., Ji, S.C., Zhang, L.S., and Zhong, J.Y., 1990, The Ailao Shan-Red River metamorphic belt: Tertiary left-lateral shear between Indochina and South China: Nature, v. 343, pp. 431–437.

Thompson, G.M., Ali, J.R., Song, X., and Jolley, D.W., 2001, Emeishan basalts, SW China: Reappraisal of the formation's type area stratigraphy and a discussion of its sigificance as a large igneous province: Journal of the Geological Society, v. 158, pp. 593–599.

Wang, L.T., Lu, Y.B., Zhao, S.J., and Luo, J.H., 1994, Permian lithofacies paleogeography and mineralization in south China: Geological Publishing House, Beijing, 147p. (in Chinese with English abstract).

White, R.S. and McKenzie, D.P., 1989, Magmatism at rift zones: the generation of volcanic continental margins and flood basalts: Journal of Geophysical Research, v. 94, pp. 7685–7729.

White, R. S. and McKenzie, D.P., 1995, Mantle plume and continental flood basalts:Journal of Geophysical Research, v. 100, pp. 17543–17585.

White, R.S., McKenzie, D., and O'Nions, K., 1992, Oceanic crustal thickness from seismic measurement and rare earth element inversion: Journal of Geophysical Research, v. 97, pp. 19683–19715.

Wignall, P.B., 2001, Large igneous provinces and mass extinctions: Earth Science Reviews, v. 53, pp. 1–33.

Wilson, J.T., 1963, A possible origin of the Hawaiian Islands: Canadian Journal of Physics, v. 41, pp. 863–870.

Xiao, L., Xu, Y.G., Mei, H.J., Zheng, Y.F., He, B., and Pirajno, F., 2004b, Distinct mantle sources of low-Ti and high-Ti basalts from the western Emeishan large igneous province, SW China: implications for plume-lithosphere interaction: Earth and Planetary Science Letters, v. 228, pp. 525–546.

Xiao, L., Xu, Y.G., Xu, J.-F., He, B., and Pirajno, F., 2004a, Chemostratigraphy of flood basalts in the Garze-Litang Region and Zangza Block: implications for western extension of the Emeishan large igneous Province, SW China: Acta Geologica Sinica, v. 78, pp. 61–67.

Xiao, L., Xu, Y.G., Chung, S.-L., He, B., and Mei, H.J., 2003, Chemostratigraphic Correlation of Upper Permian Lava Succession from Yunnan Province, China: Extent of the Emeishan Large Igneous Province: International Geology Review, v. 45, pp. 753–766.

Xu, Y.G. and Chung, S.L., 2001, The Emeishan Large Igneous Province: Evidence for mantle plume activity and melting conditions: Geochimica, v. 30, pp. 1–9 (in Chinese with English abstract).

Xu, Y.G., Chung, S.-L., Jahn, B.M., and Wu, G.Y., 2001, Petrologic and geochemical constraints on the petrogenesis of Permian-Triassic Emeishan flood basalts in southwestern China: Lithos, v. 58, pp. 145–168.

Xu, Y.G. and He, B., 2007, Thick and high velocity crust in Emeishan large igneous province, SW China: Evidence for crustal growth by magmatic underplating/intraplating, *in* Foulger, G. and Jurdy, D. eds, The origins of melting anomalies: plates, plumes, and planetary processes: Geological Society of America Special Papers (in press)

Xu, Y.G., He, B., Chung, S.L., Menzies, M.A., and Frey, F.A., 2004, The geologic, geochemical and geophysical consequences of plume involvement in the Emeishan flood basalt province: Geology, v. 30, pp. 917–920.

Xu, Y.G., Mei, H.J., Xu, J.F., Huang, X.L., Wang, Y.J., and Chung, S.L., 2003, Origin of differentiation trends in the Emeishan continental flood basalts, SW China: Chinese Science Bulletin, v. 48, pp. 390–394.

Yuan, X.C., 1995, Geophysical maps of China: Beijing, Geological Publishing House, 200 p.

Yunnan Bureau of Geology, 1990. Regional geology of Yunnan province: Geol. Mem. Series 21, Geological Publishing House, Beijing, 728 pp (in Chinese).

Zhang, Y.X., Luo, Y. and Yang, X., 1988, The Panxi Rift. Geological Publishing House, Beijing. (in Chinese).

Zhang, Z.C., Mahoney, J.J., Mao, J.W., and Wang, F.H., 2006, Geochemistry of picritic and associated basalt flows of the western Emeishan flood basalt province, China: Journal of Petrology, v. 47, pp. 1997–2019.

Zhou M.F., Malpas J., Song X., Robinson P.T., Sun M., Kennedy, A.K., Lesher C.M., and Keays R.R., 2002, A temporal link between the Emeishan large igneous province (SW China) and the end-Guadalupian mass extinction: Earth and Planetary Science Letters, 196: 113–122

Zhou, M.-F., Robinson, P.T., Lesher, C.M., Keays, R.R., Zhang, C.-J., and Malpas, J., 2005, Geochemistry, petrogenesis, and metallogenesis of the Panzhihua gabbroic layered intrusion and associated Fe-Ti-V-oxide deposits, Sichuan Province, SW China: Journal of Petrology, v. 46, pp. 2253–2280.

Zhou, M.F., Zhao, J.H., Qi, L., Su, W., and Hu, R.Z., 2006, Zircon U-Pb geochronology and elemental and Sr-Nd isotopic geochemistry of Permian mafic rocks in the Funing area, SW China, Contributions to Mineralogy and Petrology, v. 151, pp. 1–19.

Zhong, H. and Zhu, W.G., 2006, Geochronology of layered mafic intrusions from the Pan-Xi area in the Emeishan large igneous province, SW China: Mineralum Deposita, v. 41, pp. 599–606.

Zhong, H., Zhu, W.G., Chu, Z.Y., He, D.F., and Song, X.Y., 2007, Shrimp U-Pb zircon geochronology, geochemistry, and Nd-Sr isotopic study of contrasting granites in the Emeishan large igneous province, SW China: Chemical Geology, v. 236, pp. 112-133.

Yi-Gang Xu *graduated from Zhejiang University in 1987, received his Ph.D from University of Paris 7 in 1994, is now research professor of Key Laboratory of Isotope Geochronology and Geochemistry, Guangzhou Institute of Geochemistry, Chinese Academy of Sciences. His research interest includes large igneous provinces and their economic/ environmental effects, crustal and mantle composition and processes.*

Bin He *graduated from China University of Geosciences in 1984, received his Ph.D from China University of Geosciences in 2001, is now associated research professor of Key Laboratory of Isotope Geochronology and Geochemistry, Guangzhou Institute of Geochemistry, Chinese Academy of Sciences. His research interest includes geodynamics of mantle plume and its environmental effects.*

Xiao-Long Huang *received his Ph.D from the Nanjing University in 1999, is now research professor of Key Laboratory of Isotope Geochronology and Geochemistry, Guangzhou Institute of Geochemistry, Chinese Academy of Sciences. Specialized in petrology and mineralogy, his current research interest includes mineralization associated with granitic magmatism and the role of crustal-mantle interaction in the lithospheric evolution*